ARMA 12-438

Numerical modeling of volcanic slope instability and related hazards at Pacaya Volcano, Guatemala

Schaefer[1], L.N., Oommen[1], T., Corazzato[2], C. and Tibaldi[2], A. and Rose[1], W.I.
[1]*Michigan Technological University, Houghton, MI, USA*
[2]*Università degli Studi di Milano-Bicocca, Milan, Italy*

This paper was prepared for presentation at the 46th US Rock Mechanics / Geomechanics Symposium held in Chicago, IL, USA, 24-27 June 2012.

ABSTRACT: This study uses numerical modeling to determine the possibility of an edifice collapse at the active Pacaya Volcano in Guatemala. Stability analyses using the Limit Equilibrium Method (LEM) and the Finite Element Method (FEM) were performed on the south-western flank using the physical-mechanical material properties of Pacaya's intact rocks and rock mass characteristics based on field observations and laboratory tests. The Hoek and Brown failure criterion was used to calculate the friction angle, cohesion, and rock mass parameters in a determined stress range. Volcanic instability was assessed based on the variability of the Factor of Safety and Shear Strength Reduction using deterministic, sensitivity, and probabilistic analyses considering static conditions. Results indicate the volcanic slope is stable under gravity alone, but the possible presence of a layer of pyroclastics significantly reduces the stability of the slope. Future work will focus on verifying the presence of this layer and evaluating the effect of external loading mechanisms such as earthquake load and magma pressure on the slope stability at Pacaya.

1. INTRODUCTION

Volcanic landslides, which have caused over 20,000 fatalities in the past 400 years [1], are extremely hazardous geologic processes due to their size and velocity. These events can travel at speeds of 50 to 150m/s [2, 3], containing several cubic kilometers of debris and traveling tens of kilometers away from the volcano. Since the sector collapse and associated lateral eruption of Mount St. Helens in 1980, there has been a surge of interest in volcanic collapse mechanisms and collapse evidence. Collapses have now been reported at 400 volcanoes around the world, of which 21 have had a large-volume landslide (>0.1 km³) since 1500 A.D. [4]. Besides the direct impacts on nearby communities due to debris avalanches and associated lahars, they also increase the risk of explosive and/or lateral eruptions. Landslides at coastal and oceanic volcanoes can also produce tsunamis, affecting areas much farther from the volcano. Although it is difficult to predict when and where these collapses occur, geotechnical modeling can help scientists determine the probability of collapse.

2. BACKGROUND

Located 30 km south of Guatemala City (Fig. 1), Pacaya Volcano is one of the most active volcanoes in Central America, having ended a period of dormancy in 1961 and erupted as recently as summer 2010. The volcano is composed of a modern cone within the collapse amphitheater of an ancestral stratovolcano. This horseshoe-shaped scarp is the result of a sector collapse which formed a debris avalanche that traveled 25 km S-SW of the cone between 400 and 2000 years B.P. [5]. Subsequent eruptions have since built a new cone along the scarp. Since the renewal of activity in 1961, the volcano has loaded 100 to 150 m of lava flow and tephra material primarily on the SW flank of the cone. During an eruption that began in May 2010, a new vent opened outside of the scarp SE of the active cone, forming a 5 km lava flow that destroyed several houses. Concurrently, a collapse feature formed on the NW side of the modern cone and summit explosions destroyed dozens of houses several kilometers north. These coincident summit Strombolian eruptions, collapses, and flank lava eruptions suggest the possibility of magma reservoirs high in the cone, an idea that has been hypothesized previously [6, 7].

Pacaya is an ideal study site for volcanic hazard monitoring given its history of collapse, continual eruptive activity, and inherent geologic features. Furthermore, Pacaya is surrounded by several communities totaling about 9000 people that live less

than 5 km from the active cone and have been evacuated 11 times in the past 24 years [7]. Due to the combination of asymmetric loading and high magma reservoirs, one of the biggest concerns at Pacaya is related to collapse of the active cone, which would greatly expand the hazard zones. Therefore, it is critical to determine the possibility of collapse and the most important factors affecting slope stability.

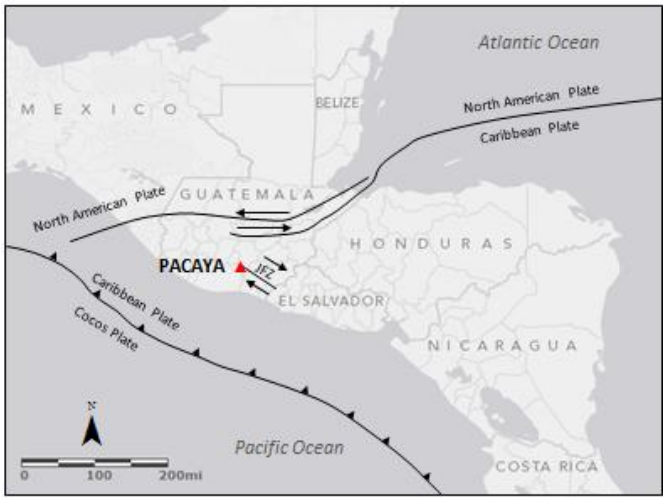

Fig. 1. Location of Pacaya Volcano along the Central American volcanic arc. JFZ denotes the Jalpatagua fault zone.

This research is modeled after Apuani, et al. (2005) [8] and Apuani and Corazzato (2009) [9], who have shown that the use of the Limit Equilibrium Method (LEM) coupled with stress-strain numerical modeling has enormous potential for understanding volcano collapse mechanisms associated with deep-seated collapses. The aims and objectives of this study include:

(i) Determine the most likely locality of slope failure through structural analysis;
(ii) Determine the physical-mechanical material properties of Pacaya's intact rocks and rock masses;
(iii) Develop a geotechnical model of the volcano using a combination of field surveys, laboratory testing, and computational modeling;
(iv) Use numerical modeling to analyze areas of interest;
(v) Understand the mechanisms and destabilizing factors that could lead to a large-scale collapse.

3. STRUCTURAL ANALYSIS

Structural surveys were performed in the field to determine the local stress regime and most likely location of slope failure. Along the scarp, 150 joints were measured and grouped into joint sets K1, K2, K3, and K4 based on their geometry (strike, dip, and inclination) (Fig. 2-A). The southern portion of Guatemala is located on the Caribbean tectonic plate (Fig. 1), which is subject to E-W crustal extension as evidenced by the existence of a series of N-S trending grabens [10]. The SE corner is also split by the right-lateral strike-slip Jalpatagua fault zone. Acting together, Escobar Wolf [11] suggests that the volcano is undergoing both NW-SE strike-slip and E-W tensional stresses (orientation of mapped faults from this report, Fig. 2-B). This stress combination results in a NNW-SSE transtensional regional regime for Pacaya, with the minor principal stresses (σ'_3) oriented ENE-WSW (Fig. 2-C).

These two components are reflected in the jointing patterns seen along the scarp, with K1 reflecting the regional strike-slip component and K2 reflecting the regional tensional stress component. The geometry of joint groups K3 and K4 are not seen regionally, described by Vallance et al. [5] indicating that the ancient collapse caused a re-orientation of local stress fields as adjacent material was removed in the avalanche.

Orientation of volcanic craters (including the currently active and ancestral Cerro Chino vents) new vents, and the 2010 collapse feature are also aligned in this NNW-SSE pattern (Fig. 3), suggesting this stress regime is responsible for much of the volcano's growth pattern, including the SW orientation of the ancestral collapse. The regional and local stress patterns both suggest the most likely direction of a future collapse to be aligned roughly NE-SW. A large lava dome on the NE flank of the volcano is likely acting as a restricting weight and this, paired with recent loading of lava flow material on the SW flank, and suggests that the most likely direction for a future collapse will be to the SW.

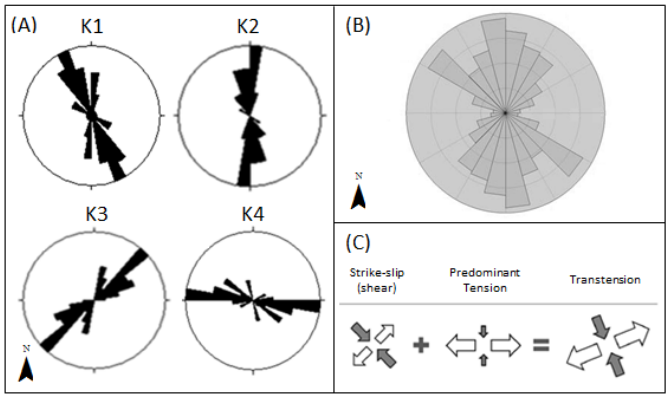

Fig. 2. Orientation of mapped joints and faults around Pacaya and the possible stress state of the volcano based on local and regional stress patterns. (A) Results of structural field surveys performed along the ancient fault scarp, with joints grouped into four sets. (B) Orientation of mapped faults within 50 km of Pacaya that reflect both the strike-slip and tensional regional stress regimes (Courtesy of Escobar Wolf, 2012). (C) Possible stress state at Pacaya, suggesting future collapse to be oriented SW.

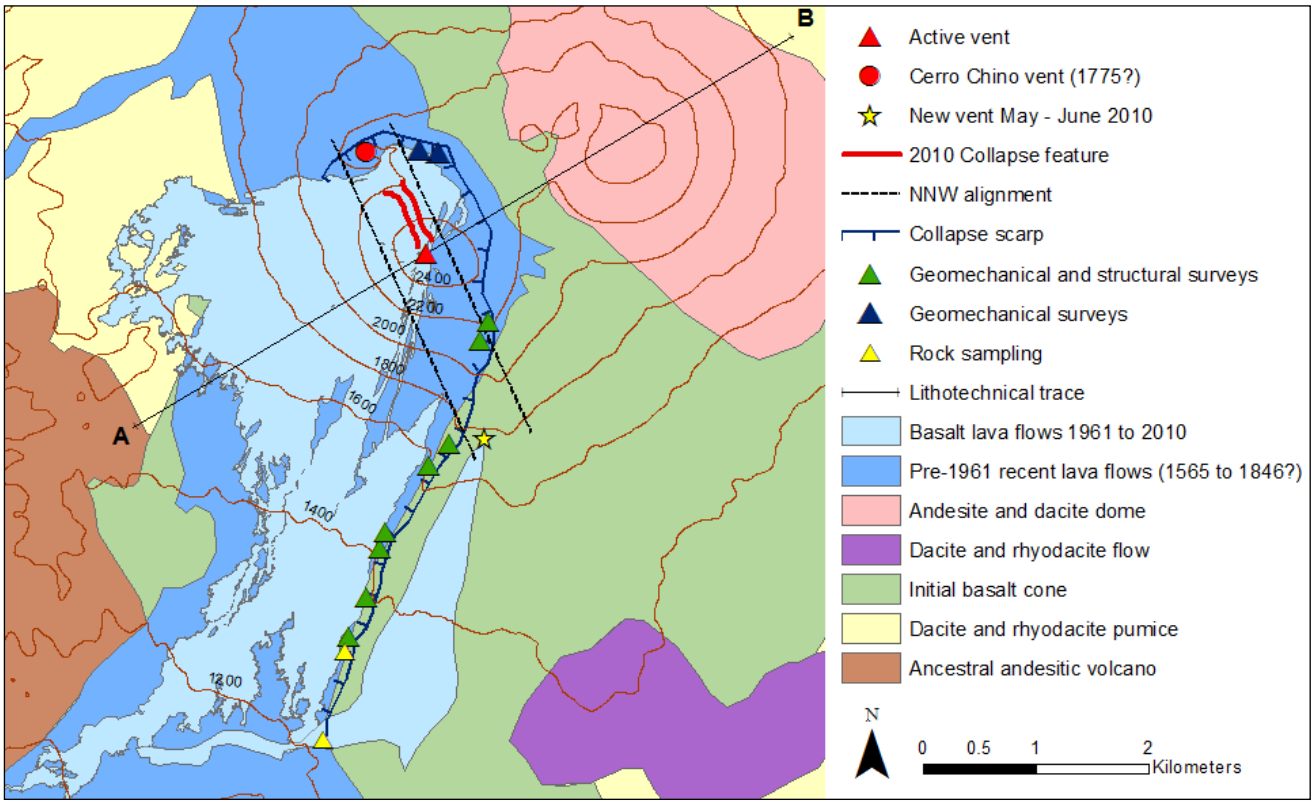

Fig. 3. Simplified geologic map of Pacaya and location of field sites. General geology modified from IGN / Eggers [12].

4. ROCK MASS PROPERTIES

Both the modern and initial cones are composed of predominately interbedded lava, breccia, and pyroclastics formed of porphyritic olivine basalt. For numerical modeling purposes, the different lithostratigraphic units can be categorized into lithotechnical units according to their mechanical characteristics. Based on field observations, the rock masses at Pacaya were grouped into five lithotechnical units considering their percentages of lava versus breccia deposits:

(i) Lava (L): predominately lava (>80%) alternating with autoclastic breccia layers;
(ii) Lava-Breccia (LB): alternating lava (50-80%) and breccia layers;
(iii) Breccia-Lava (BL): alternating breccia (>50%) and lava layers;
(iv) Breccia (B): predominately breccia (>80%) alternating with lava layers;
(v) Pyroclastic (P): prevailing pyroclastics.

Structural and geomechanical surveys and tests were performed at 10 outcrops along the collapse scarp (Fig. 3). Because of the complexity in addressing the strength of rock masses, especially in situations where rock mass "quality" can range from poor to very good (i.e. pyroclastics versus lava rocks), this study adopted the Geological Strength Index (GSI) introduced by Hoek (1994) [13] and developed by Hoek and Marinos (2000) [14] to characterize and evaluate the strength of the large variety of rock mass types found at Pacaya.

4.1. Physical and Mechanical Properties

To input lithotechnical unit properties for numerical modeling, the intact rock and rock mass parameters must be described in accordance with engineering material properties. Rock mass quality was assessed with the GSI using visual characterizations of the rock structures and surface conditions (Fig. 4). Lava rocks had the highest GSI range of 55-70, with LB(45-60), BL(35-50), B(25-40) and P(8-20) progressively degrading in surface quality and structural integrity. Measurements of intact rock strength were made using Schmidt hammer rebound values and uniaxial compressive laboratory tests. Schmidt hammer rebound tests were repeated 20 times at each survey site and an average value was taken. These values were converted to equivalent uniaxial compressive strength (σ_{ci}) values using the following empirical correlation:

$$\sigma_{ci} = 2.75 \cdot N - 36.83 \qquad (1)$$

obtained exclusively from testing volcanic rocks [15], with N being the Schmidt hammer rebound value. Using this relation, the uniaxial compressive strength averaged 88.03 MPa for lava rock and 29.92 MPa for breccia rock (Table 1).

Table 1. Uniaxial compressive strength (σ_{ci}) of volcanic samples from Schmidt hammer and uniaxial compressive tests. Values are given as the mean ± the standard deviation.

	Schmidt Hammer		Laboratory uniaxial tests		
Sample	*n*	σ_{ci} (Mpa)	*n*	σ_{ci} (Mpa)	Unit Weight (kN/m³)
Lava	18	88.03 ± 29.92	12	47.62 ± 16.01	26.82 ± 0.11
Breccia	10	47.6 ± 11.97	17	33.08 ± 11.26	22.92 ± 0.91

Additionally, two intact rock samples, one lava and one breccia, were collected from the collapse scarp for laboratory measurements of unit weight (γ) and intact rock uniaxial compressive strength. Standard uniaxial compressive tests were completed on 12 lava and 17 breccia cores obtained from the two field samples (Table 1). Lab results are significantly lower than compressive strength values obtained using the Schmidt hammer, with lava rock averaging 47.62 MPa and breccia averaging 33.08 MPa. This pattern in similar to those found by other authors [16] and could possibly be attributed to vesicularity or small number of samples tested. Additionally, unit weight (γ) values were calculated, with lava rock averaging 26.82 kN/m^3 and breccia rock averaging 22.92 kN/m^3.

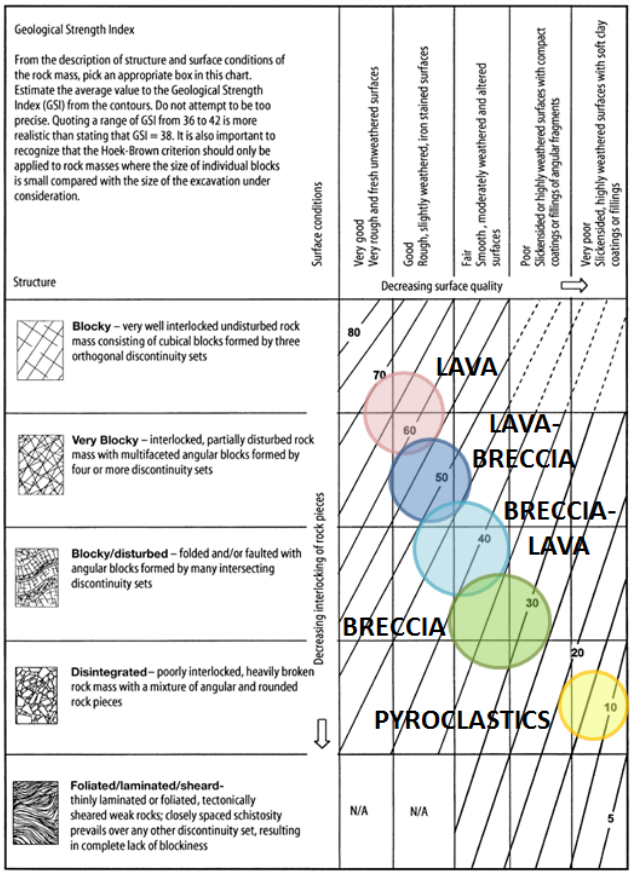

Fig. 4. Geological Strength Index (GSI) ranges of the lithotechnical units at Pacaya. The GSI classifies rock masses based on structural characteristics and surface conditions. Classification table from Marinos and Hoek [14].

4.2. Rock Mass Strength

Rock mass strength was evaluated using Hoek and Brown's non-linear strength law [13]. The parameters involved in the analysis include: uniaxial compressive strength of the rock mass (σ_{ci}); material constant (m_i) that describes the petrology and texture of the intact rock; GSI of the rock mass; and the disturbance factor (D). Parameter D depends on the degree of disturbance to which the rock mass has been subjected by blast damage. For this study, D = 0 since the outcrops are in situ rock masses. The Hoek and Brown failure criterion for jointed rock masses has the form:

$$\sigma'_1 = \sigma'_3 + \sigma_{ci} \cdot \left(m_b \cdot \frac{\sigma'_1}{\sigma_{ci}} + s \right)^a \qquad (2)$$

where σ'_1 and σ'_3 are the maximum and minimum effective stresses at failure, σ'_{ci} is the uniaxial compressive strength of the intact rock, s and a are constants that depend upon joint conditions and the degree of fracturing for the rock mass, and m_b is a reduced material constant for the rock mass expressed as

$$m_b = m_i \exp\left(\frac{GSI - 100}{28 - 14D} \right) \qquad (3)$$

Table 2 summarizes the ranges and values chosen as input data (in brackets) for numerical modeling. These values were based on other author's suggestions [16] and are either the predominate or lowest values based on field observations and laboratory tests. The physical-mechanical properties include both the Hoek-Brown rock mass properties necessary for the failure criterion and the calculated Mohr-Coulomb equivalent parameters necessary for FEM analysis. The Mohr-Coulomb parameters were calculated using Rocscience RocLab 1.0 [17]. In considering the Hoek-Brown to Mohr-Coulomb relationship, it is necessary to specify a range for the upper limit of confining stress (σ'_{3max}) [18]. For Pacaya, this was calculated using Rocscience Phase2 8.0 [17] using an empirical relationship considering the height of the slope and the unit weight of the rock mass, resulting in a range of σ'_{3max} = 5-15 MPa. No pyroclastics were tested for unit weight, therefore data from the literature was used [8]. Because the Lava-Breccia and Breccia-Lava lithotechnical units have percentages of both rock types, the physical-mechanical properties were calculated from known values of Lava and Breccia rock.

5. GEOTECHNICAL MODEL

A geotechnical model of the volcano was constructed to be used in modeling (Fig. 5). The cross-sectional geometry of this section was obtained from Digital Elevation Models (DEMs) from 1954 [19] and 2001

Table 2. Physical and mechanical properties of the lithotechnical units.

	Lava	Lava-Breccia	Breccia-Lava	Breccia	Pyroclastics
Hoek-Brown failure criterion rock mass properties.					
Intact rock- σci (MPa)	26-142 (63)^{Lb,S}	52^{S}	42^{S}	14-55 (33)^{Lb,S}	10-20 (20)^{S}
Geological Strength Index- GSI	55-70 (65)^{S}	45-60 (50)^{S}	35-50 (40)^{S}	25-40 (35)^{S}	8-20 (15)^{S}
mi	25 ± 5 (25)^{Tr}	22 ± 5 (22)^{Tr}	19 ± 5 (19)^{Tr}	19 ± 5 (19)^{Tr}	13 ± 5 (13)^{Tr}
Disturbance factor- *D*	0^{S}	0^{S}	0^{S}	0^{S}	0^{S}
Unit weight- γ (kN/m³)	26.56-26.98 (26.82)^{Lb}	25.65	24.39	22.01-23.83 (22.92)^{Lb}	8-20 (15)*
S in situ direct tests and evaluations, *un* uncertain data, *Tr* theoretical data, *Lb* laboratory results.					
* based off of Apuani et al. (2005). Values chosen for input data in brackets when ranges are given.					
Mohr-Coulomb equivalent parameters calculated using Rocscience RocLab 1.0. Range of σ'_{3max} = 5-15 MPa.					
mb	7.163	3.689	2.23	1.865	0.625
s	0.021	0.004	0.0013	0.0007	0.0001
a	0.502	0.506	0.511	0.516	0.561
Apparent cohesion- c (MPa)	2.4-4.9	1.7-3.6	1.3-2.8	1.13-2.4	0.53-1.09
Friction angle- φ (°)	52.1-43.3	45.3-36.1	39.2-30.1	35.6-26.8	21.9-15.6
Tensile strength- σ'tm (MPa)	-0.18	-0.054	-0.024	-0.014	-0.003
Uniaxial compressive strength- σm (MPa)	8.944	3.132	1.389	0.843	0.1
Global strength- σ'cm (MPa)	23.268	13.273	8.086	6.027	1.552
Young's Modulus- *E* m (MPa)	7581	3686	1916	1361	437

[20]. The lithotechnical units were then assigned based on field observations and geological maps [12]. Although there are no outcrops in the chosen cross-section, the lithotechnical units outcropping throughout the scarp of the volcano can be projected and used as a good indication of the interior patterns of the volcano. The recently erupted material is highly autobrecciated and therefore assigned as lithotechnical unit BL. The most prevalent percentage of lava to breccia along the scarp is represented by unit LB, which was assumed to compose the majority of the edifice. A thick layer of dacite pumice covers the area from past caldera eruptions ranging from 10 to 200 m in depth [21]. Recent eruption deposits contain pieces of this layer, suggesting the pyroclastics do exist beneath the main edifice. Additionally, this layer outcrops around the main volcanic units (Fig. 3), including on both ends of the cross section. The depth of the pyroclastics beneath Pacaya is unknown, therefore two models were tested: one with a 10 m layer of pyroclastics, and one without.

6. NUMERICAL MODELING

Volcano slope stability was analyzed using Limit Equilibrium Methods (LEM) in Rocscience Slide 6.0 for calculating slip surfaces. Additionally, stresses in the slope were calculated using two-dimensional, elasto-plastic Finite Element Methods (FEM) in Rocscience Phase2 8.0 [17]. As stated in Section 5, two models were evaluated: (A) with a 10 m layer of pyroclastics beneath the edifice; (B) without a layer of pyroclastics. For deterministic trials, the physical and mechanical properties of the lithotechnical units stayed constant.

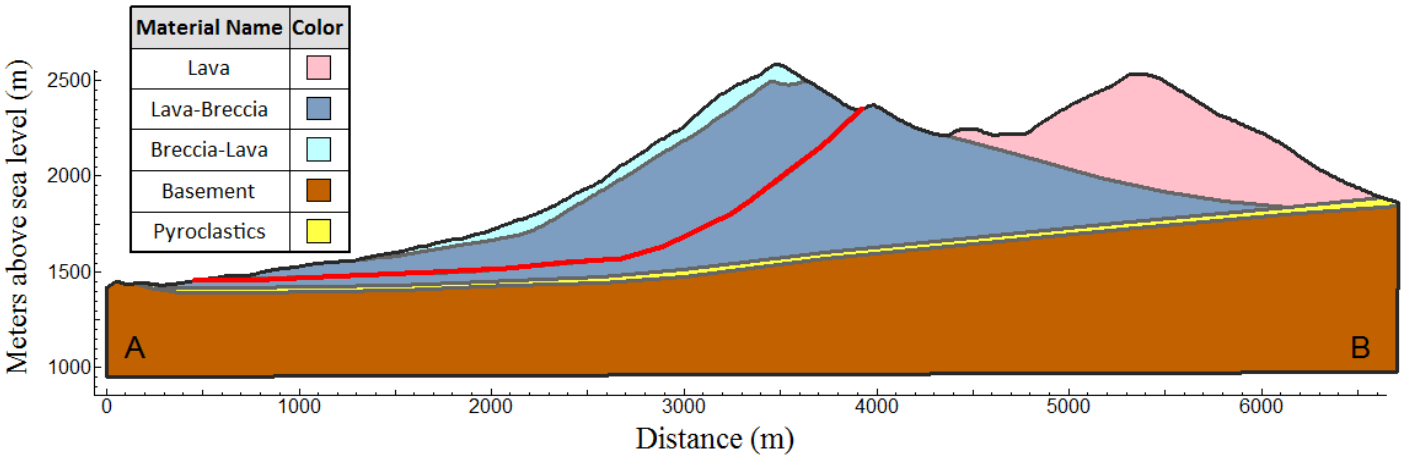

Fig. 5. Lithotechnical section of Pacaya with assigned lithotechnical units (trace A-B in Fig.1). Past collapse geometry interpreted in red based on projection of the collapse scarp.

In LEM analysis, slip surfaces were found using Janbu Simplified method and an auto-refined, non-circular search method considering deep failure surfaces of 200 meters in depth or greater. The outcome for LEM analysis is the Factor of Safety (FS), which describes the stability of the slope. Because of the presence of weak rocks and complex interior magmatic plumbing systems in volcanic environments, the slope can be assessed as stable (FS>1.5), moderately unstable (1.3<FS<1.5), inherently unstable (1<FS<1.3) or unstable (FS<1) [22]. FEM analysis was used to better understand the progressive evolution of the failure surface and the location of maximum shear strain. The outcome is the critical Shear Strength Reduction (SSR) factor, which is equivalent to FS values. The same model properties from LEM analysis were used in FEM.

In this study, the stability of the volcanic slope is analyzed as a two-dimensional (2D) plane strain problem. Previous studies have shown that this assumption provides a lower estimate of stability/factor of safety compared to the three-dimensional (3D) analysis [23]. However, future studies would consider the 3D effects to better constrain the out of plane extent and volume of potential slope instability.

For models A and B (see Table 4), the uniaxial compressive strength and unit weight parameters of the LB unit were assessed using a sensitivity analysis which varies one variable at a time within a range while keeping all other variables constant. Unlike a deterministic analysis that assumes the input parameters are correct, this takes into account uncertainties in these parameters. A probabilistic analysis was conducted for both models using the Monte Carlo sampling technique to assign statistical distributions to the model input parameters to account for random behavior in the slope stability problem. The results are displayed as a cumulative probability curve, where each point gives the probability that the FS value will be less than or equal to its value at that point.

Table 3. Input values for sensitivity and probabilistic analysis of the Lava-Breccia unit.

Parameter	Unit	Distribution	Mean	Standard Deviation	Absolute minimum	Absolute maximum
Uniaxial compressive strength (σ_{ci}): Lava-Breccia	MPa	Normal	52	23	1	100
Unit weight (γ): Lava-Breccia	kN/m^2	Normal	25.65	2	10	30

7. RESULTS

The inclusion of a pyroclastics unit beneath the edifice greatly affects the geometry of the slip surface and the amount of material predicted to fail. The difference in both slip surface geometry and area of maximum strain are shown in Fig. 6 for LEM analysis and Fig. 7 for FEM analysis.

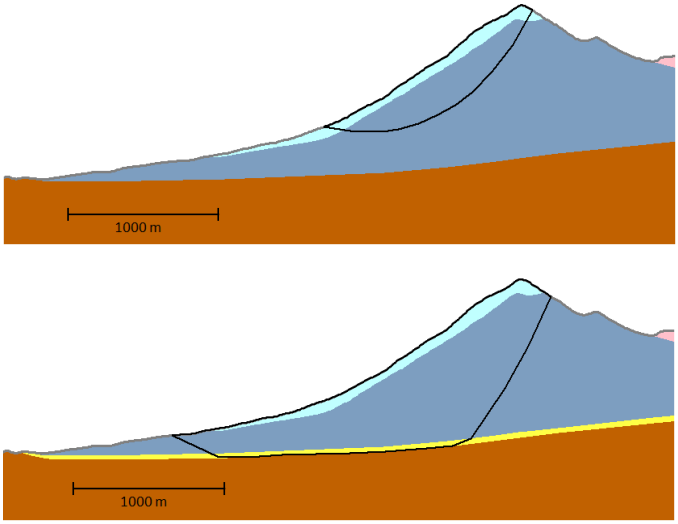

Fig. 6. Changes in the slip surface geometry due to the presence of the pyroclastics unit beneath the edifice for LEM analyses. The model without pyroclastics (top) shows a much shallower slip surface, while the model with a pyroclastics layer (bottom) shows a much larger slip surface that fails along the bottom of this weak layer.

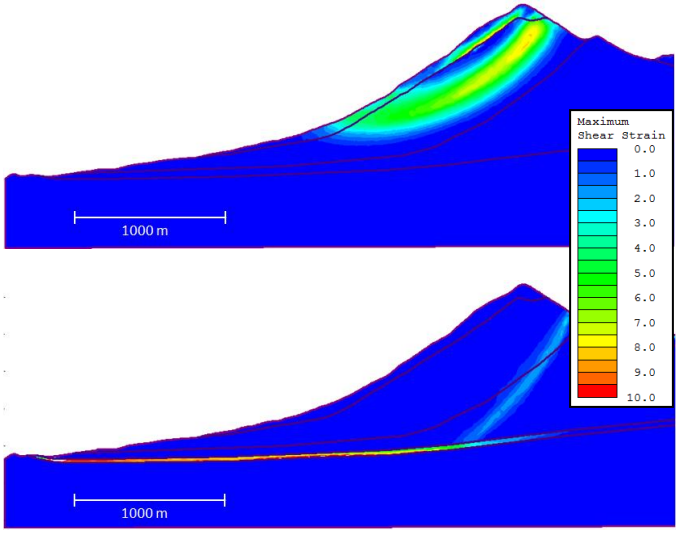

Fig. 7. Effect of the pyroclastic unit on the location of maximum shear strain in FEM analyses mimic LEM geometry changes. The model without the pyroclastics layer (top) shows multiple shallow strain surfaces, while the model with a pyroclastics layer (bottom) shows a deeper strain surface that is confined to the pyroclastics unit.

SSR values are in good agreement with the FS values for each scenario. Both FS and SSR results for the minimum slip surface are significantly reduced with the presence of the pyroclastics layer (Table 4). Additionally, FEM results show maximum shear strain contours with similar geometries to the slip surfaces found in LEM analyses (Fig. 7). In models that contained the pyroclastics unit,

the strain was concentrated deeper in the edifice and throughout the pyroclastics, whereas the models without showed multiple, shallower strain surfaces.

Table 4. FS and SSR results for deterministic trials.

Model	Pyroclastics unit?	Factor of Safety	Shear Strength Reduction
A	Yes	1.821	1.98
B	No	2.539	2.6

In static conditions, the slope is always stable (FS and SSR values>1.5). Sensitivity analysis shows that material properties would have to be reduced to unrealistic values to induce the slope to fail (Fig. 8, 9). In the model with the pyroclastics unit, the model most likely to fail, the uniaxial compressive strength value for the LB unit would have to be reduced from 52 to 1.95 MPa for FS<1 - a reduction of over 96%. This suggests that the slope is highly unlikely to have a catastrophic failure unless affected by an external mechanism.

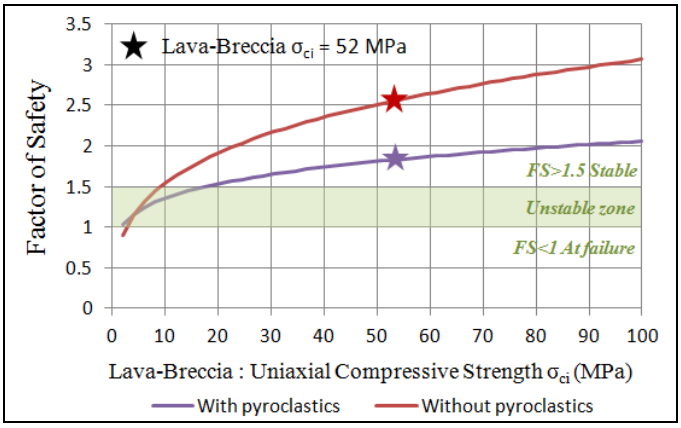

Fig. 8. Sensitivity analysis shows the uniaxial compressive strength would have to be reduced to unrealistic values to induce failure.

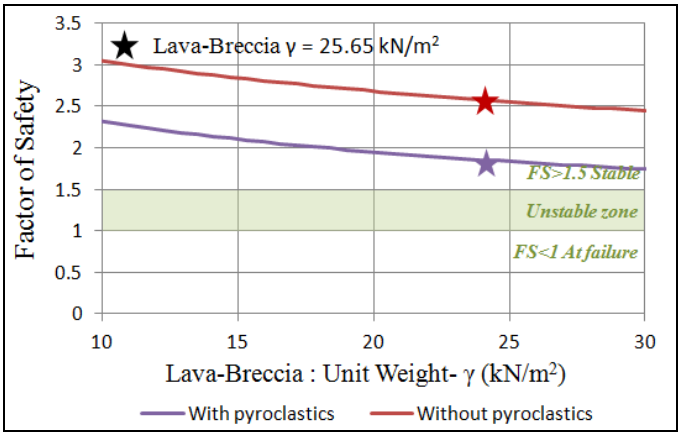

Fig. 9. Sensitivity analysis shows that variability in the unit weight within realistic values will not cause instability.

8. CONCLUSION

Slope instability is very complex in volcanic environments. They are typically heterogeneous- with complex magmatic systems and frequent changes in morphology. Because of this, several assumptions and simplifications have been made that are reasonable and which fit the purpose of this conceptual modeling. These include the geotechnical properties, and the model's geometry and geological features.

FS and SSR results suggest that the slope is stable under static conditions. Probabilistic analysis shows that in both model conditions with and without a layer of pyroclastics, the probability is very low for the FS to reach critical values (Fig. 10). Sensitivity analysis of uniaxial compressive strength and unit weight additionally show that these properties would have to be reduced to unrealistic values to induce slope failure. Therefore, in considering poor mechanical properties or a drastic reduction in rock properties (i.e. through hydrothermal alteration), gravitational forces are not enough to induce failure as a single mechanism.

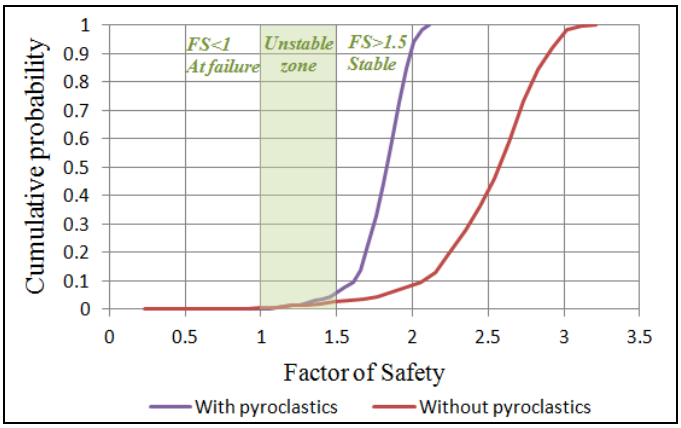

Fig. 10. Probabilistic analysis of both model conditions suggest a very low probability for the edifice to collapse under current conditions.

Slip surface geometries found in the models with the layer of pyroclastics beneath the edifice are more similar to the estimated geometry of the ancestral collapse (Fig. 5) than those without. This strongly suggests that this layer was a mechanism which controlled the ancestral failure. Additionally, models with the pyroclastics layer have a higher probability of reaching instability than those without (Fig. 10). Therefore, it is important to determine the extent of the pyroclastics unit and to derive better estimates of its thickness beneath the edifice.

FEM results are in good agreement with LEM results, both in comparing maximum shear strain contours to slip surface geometries and SSR to FS values. Maximum shear strain contours show multiple regions of deep

deformation, suggesting the possibility of a large sector collapse under the right conditions. Future work will consider the addition of magmatic and seismic forces as possible triggering mechanisms for a large-scale collapse.

9. REFERENCES

1. Siebert, L., H. Glicken, and T. Ui. 1987. Volcanic hazards from Bezymianny- and Bandai-type eruptions. *Bulletin of Volcanology*, 49: 435-459.
2. Ui, T., H. Yamamoto, and K. Suzuki. 1986. Characterization of debris avalanche deposits in Japan. *J. Volcanol. Geotherm. Res.*, 29: 231-243.
3. Siebert L., J.E. Béget, and H. Glicken. 1995. The 1883 and late-prehistoric eruptions of Augustine volcano, Alaska. *J. Volcanol. Geotherm. Res.*, 66: 367-395.
4. Carrasco-Núñez, G., L. Siebert, and L. Capra. 2011. Hazards from volcanic avalanches. *Horizons in Earth Science Research*, 3: 199-227.
5. Vallance, J.W., L. Siebert, W.I. Rose Jr., J. Raul Girón, and N.G. Banks. 1995. Edifice collapse and related hazards in Guatemala. *J. Volcanol. Geotherm. Res.*, 66: 337-355.
6. Eggers, A. 1983. Temporal gravity and elevation changes at Pacaya volcano, Guatemala. *Journal of Volcanology and Geothermal Research*, 19: 223 – 237.
7. Matías Gómez, R.O. 2009. Volcanological map of the 1961-2009 eruption of Volcán de Pacaya, Guatemala. MS thesis, Michigan Technological University, Houghton, MI.
8. Apuani, T., C. Corazzato, A. Cancelli, and A. Tibaldi. 2005. Physical and mechanical properties of rock masses at Stromboli: a dataset for volcano instability evaluation. *Bull. of Eng. Geo. & the Env*., 64: 419-431.
9. Apuani, T. and C. Corazzato. 2009. Numerical model of the Stromboli volcano (Italy) including the effect of magma pressure in the dyke system. *Rock Mechanics and Rock Engineering*, 42: 1, 53-72.
10. Burkhart, B. and S. Self. 1985. Extension and rotation of crustal blocks in northern Central America and effect on the volcanic arc. *Geology*, 13: 22-26.
11. Escobar Wolf, R. 2012. The eruption of Volcán de Pacaya on May-June, 2010. Unpublished report.
12. IGN / Eggers, A., 1969, Mapa Geologico de Guatemala Escala 1:50,000. Hoja 2059 II G, "Amatitlan". First edition (map). Guatemala.
13. Hoek, E. 1994. Strength of rock and rock masses. *ISRM News Journal*, 2(2): 4-16.
14. Marinos, P. and E. Hoek. 2000. GSI – A geologically friendly tool for rock mass strength estimation. *Proc. GeoEng2000 Conference*, Melbourne.
15. Dinçer, I., A. Altay, I. Çobanoglu, Y. Uras. 2004. Correlation between Schmidt hardness, uniaxial compressive strength and Young's modulus for andesites, basalts, and tuffs. *Bull. Eng. Geol. Env.*, 63: 141-148.
16. del Potro, R. and M. Hürlimann. 2008. Geotechnical classification and characterization of materials for stability analyses of large volcanic slopes. *Eng. Geo.*, 98: 1-17.
17. Rocscience Inc. 2012. RocLab v1.0, Phase2 v8.0, and Slide v. 6.0 software. Toronto, Canada.
18. Hoek, E., C. Carranza-Torres and B. Corkum. 2002. Hoek-Brown failure criterion – 2002 Edition. *Proc. NARMS-TAC Conference*, 1: 267-273.
19. U.S. Geological Survey (USGS) Cascades Volcano Observatory. 2001. Colomba_hp = 1:50,000-scale hypsography (contours) for Quetzaltenango quadrangle, Guatemala. Metadata.
20. JICA, INSIVUMEH, and SEGEPLAN, 2003, Estudio del establecimiento de los mapas basicos y de amenaza para el sistema de información geográfica de la República de Guatemala. Final report executive abstract (unpublished): 206.
21. Eggers, A.A. 1971. *The geology and petrology of the Amatitlán Quadrangle, Guatemala.* MS Thesis. Michigan Technological University, MI.
22. Hoek, E. 2007. *Practical Rock Engineering*. PDF, 2007 edition: www.rocscience.com/education/hoeks_corner
23. Michalowski, R.L. 2010. Limit Analysis and Stability Charts for 3D Slope Failures. *J. Geotech. Geoenviron. Eng*., 136, 583.